



COMET: BENCHMARK FOR COMPREHENSIVE BIOLOGICAL MULTI-OMICS EVALUATION TASKS AND LANGUAGE MODELS

Anonymous authors

Paper under double-blind review

ABSTRACT

As key elements within the central dogma, DNA, RNA, and proteins play crucial roles in maintaining life by guaranteeing accurate genetic expression and implementation. Although research on these molecules has profoundly impacted fields like medicine, agriculture, and industry, the diversity of machine learning approaches—from traditional statistical methods to deep learning models and large language models—poses challenges for researchers in choosing the most suitable models for specific tasks, especially for cross-omics and multi-omics tasks due to the lack of comprehensive benchmarks. To address this, we introduce the first comprehensive multi-omics benchmark COMET (Benchmark for Biological **CO**mprehensive **M**ulti-omics **E**valuation **T**asks and Language Models), designed to evaluate models across single-omics, cross-omics, and multi-omics tasks. First, we curate and develop a diverse collection of downstream tasks and datasets covering key structural and functional aspects in DNA, RNA, and proteins, including tasks that span multiple omics levels. Then, we evaluate existing foundational language models for DNA, RNA, and proteins, as well as the newly proposed multi-omics model, offering valuable insights into their performance in integrating and analyzing data from different biological modalities. **We observed that DNA, RNA, and protein models can be applied to tasks across different omics by leveraging initialized embeddings, with protein models demonstrating superior performance across various omics. Through the evaluation of multi-omics tasks, we identified significant gaps in the capabilities of current models to address these challenges, highlighting substantial opportunities to enhance multi-omics integration and improve overall performance.**

1 INTRODUCTION

Driven by curiosity about uncovering the fundamental principles of life sciences, humans have never ceased exploring the microscopic mechanisms of biological processes. DNA, RNA, and proteins, as fundamental molecules of the central dogma (Crick, 1970), play critical roles in sustaining life. Through their interrelated functions, they ensure the accurate expression and execution of genetic instructions, making them central to all biological processes. Current research on these three types of molecules has already had widespread and profound impacts across multiple fields. For example, gene sequencing and editing technologies have made early diagnosis and treatment of hereditary diseases possible (Le, 2020). Genetic modification has enabled efficient and targeted crop improvement (Ahmar et al., 2020). The analysis of protein structure and function has driven advancements in targeted drug design and the application of industrial enzymes (Śledź & Cafilisch, 2018; Chapman et al., 2018). Consequently, deepening our understanding of how these molecules interact and function is crucial for unraveling the complex mechanisms underlying biological processes and driving technological and application advancements in agriculture, industry, and medicine.

Despite significant advances, current research on biological molecules faces significant challenges. With the development of machine learning technologies, research methodologies have evolved from traditional statistical approaches (Karollus et al., 2021; Bhasin et al., 2005; Kathuria et al., 2018) to deep learning models (Bogard et al., 2019; Zhuang et al., 2019; Zhang et al., 2020) and, more recently, to large language models (Chen et al., 2022; Zhou et al., 2023; Rives et al., 2021). However, this diversity of approaches has made it challenging for researchers to choose the most suitable

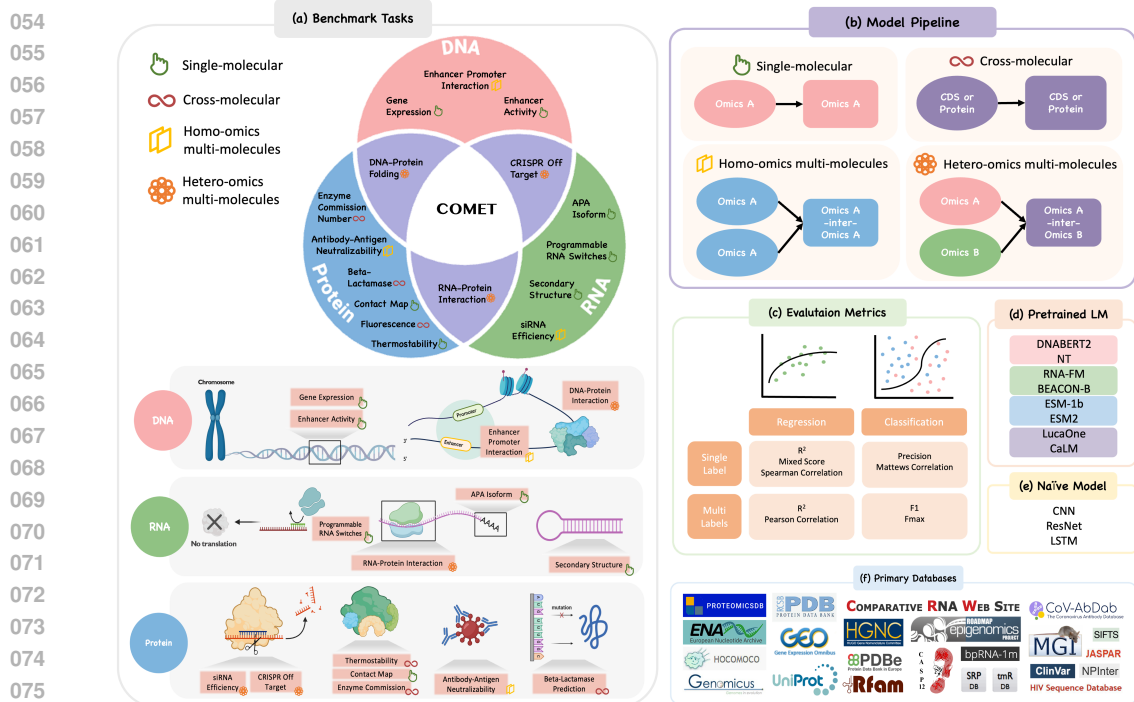


Figure 1: **Overview of COMET.** (a) **Benchmark Tasks:** The tasks are organized into four categories based on omics data: DNA, RNA, protein and multi-omics. They are further classified into single-molecular, cross-molecular, homo-omics multi-molecules and hetero-omics multi-molecules specified by icons to indicate the type of omics and interaction involved. (b) **Model Pipeline:** The benchmark evaluates model across four task types. Single molecular tasks have inputs and downstream task contained within a single omics type. Cross-molecular tasks utilize either CDS or protein data to perform downstream task involving the other. Homo-omics multi-molecules tasks involve two molecular interactions within the same omics type. Hetero-omics multi-molecules tasks refer to interactions spanning two omics types A.I. (c) **Evaluation Metrics:** Tasks are grouped into four by number of labels and supervised tasks types. Within each, tasks are evaluated with diverse metrics shown. (d) **Pretrained LM and (e) Naive Model:** Shows the pretrained omics language models and naive supervised models we used as baselines. (f) **Primary Databases:** Lists the primary data source we adopted and processed for our model training and evaluation.

model for their specific tasks. To address this issue, kinds of benchmarks have been established for specific scenarios. For example, benchmarks like BEND (Marin et al., 2023), BEACON (Ren et al., 2024) and PEER (Xu et al., 2022) have been developed specifically for DNA, RNA and protein-related tasks. These benchmarks serve as reference points for evaluating models in the specific domain, helping researchers compare performance across different methods and choose the most suitable approaches for their work.

Inspired by the unified models in the NLP field (Ray, 2023), scientists are now striving to develop foundational models capable of integrating different omics data in biology. This has led to growing interest in cross-omics and multi-omics research. By exploring the relationships between multi-omics data, they aim to uncover deeper insights into biological processes and foster innovation across research and application domains (Outeiral & Deane, 2024; He et al., 2024). However, as previously mentioned, the community still lacks a comprehensive benchmark for evaluating cross-omics and multi-omics tasks. Such a benchmark is essential for clearly defining the critical issues in multi-omics research and guiding its future direction.

Therefore, we propose a comprehensive benchmark called COMET (Benchmark for Biological **C**omprehensive **M**ulti-omics **E**valuation **T**asks and **L**anguage **M**odels) for the evaluation of single-omics, cross-omics, and multi-omics biological tasks. We select key single-omics tasks from DNA, RNA, and proteins covering structure, function and engineering, allowing for a thorough assessment of the models’ performance in specific contexts. In addition, we collect the corresponding codon sequences for proteins and several downstream tasks that span multiple omics. For the models, we

108 select two key foundational models from each omics field, and test the newly proposed multi-omics
109 method LucaOne (He et al., 2024). The benchmark allows for a deeper understanding of models
110 performance in integrating and analyzing data from different biological modalities.

111 Through the observation of our experimental results, we surprisingly find that using models from
112 other modalities can achieve comparable performance. For example, DNA/RNA models can per-
113 form protein tasks well. Additionally, we discovered that pretrained protein language models and
114 multi-omics models have strong potential for multi-molecule understanding. To the best of our
115 knowledge, we are the first to propose a comprehensive biological multi-omics benchmark, aimed
116 at evaluating models across single-omics, cross-omics, and multi-omics tasks. The overview of
117 COMET is shown in Figure 1. Our contributions can be summarized as follows:

- 118 • We build the first comprehensive biological multi-omics benchmark, covering key struc-
119 tural and functional tasks and data in single-molecules, and compiling tasks and data in-
120 volving cross-molecules and multi-molecules.
- 121 • We evaluate existing foundation models for DNA, RNA, and proteins, as well as multi-
122 omics approaches. We conduct experiments with fully-finetuned or frozen models. This
123 provides a reference for researchers in selecting methods with appropriate finetuning ways.
- 124 • We design various approaches to evaluating cross-omics and multi-omics, bridging the gap
125 between different omics. We find that different omics models can benefit other types of
126 omics tasks and multi-molecular tasks still present significant challenges to face.

128 2 RELATED WORK

129 **Biology language models.** The rapid evolution of biology language models has significantly ad-
130 vanced computational biology by leveraging natural language processing techniques to analyze bi-
131 ological sequences. DNABERT (Ji et al., 2021), DNABERT2 (Zhou et al., 2023), the Nucleotide
132 Transformer (Dalla-Torre et al., 2023) and Genomics-FM (Ye et al., 2024) adapt the BERT archi-
133 tecture for DNA sequences, but differ primarily in terms of tokenizer design, model parameters
134 and pre-trained data. HyenaDNA (Nguyen et al., 2024) models long-range dependencies at single-
135 nucleotide resolution. The emergence of foundational RNA models, including RNA-FM (Chen
136 et al., 2022), BEACON-B (Ren et al., 2024) and UTR-LM (Chu et al., 2024) utilize sophisticated
137 language modeling techniques. These models have demonstrated the ability to address a wide array
138 of RNA-related tasks, thereby offering deeper insights into RNA biology. In protein analysis, The
139 ESM family (Rives et al., 2021; Meier et al., 2021; Lin et al., 2023; Hayes et al., 2024) highlights
140 the impact of scaling unsupervised learning through the use of large protein sequence datasets and
141 a transformer-based architecture capable of capturing complex dependencies within sequences. For
142 multi-omics models, LucaOne (He et al., 2024) and CD-GPT (Zhu et al., 2024) unify nucleic acid
143 and protein data, while differ in training method. In the realm of cross-omics, Calm (Outeiral &
144 Deane, 2024) introduces codon embeddings to protein language models, enhancing predictive per-
145 formance by leveraging biological data containing richer signals. Boshar et al. (2024) explore the
146 efficacy of genomic language models on protein tasks. Prakash et al. (2024) explore the possibility
147 of applying pre-trained DNA and protein models to RNA tasks. These advancements underscore the
148 transformative potential of large-scale language models in decoding genomic, transcriptomic, and
149 proteomic complexities, fostering breakthroughs in molecular biology, and protein science.

150 **Benchmarks in biological language.** In the field of biological language processing, benchmarks
151 have been instrumental in driving advancements across various molecular research areas. For DNA,
152 significant contributions include Genomic Benchmarks (Grešová et al., 2023) and BEND (Marin
153 et al., 2023), which collect diverse DNA tasks like gene finding, enhancer annotation, and CpG
154 methylation. (Kao et al., 2024) introduces the evaluation of models for long-range tasks. Rn-
155 aBench (Runge et al., 2024) primarily focuses on RNA secondary structure and design tasks. BEA-
156 CON (Ren et al., 2024) is introduced to evaluate language models on RNA tasks and proposes a
157 strong baseline model called BEACON-B. Protein benchmarks such as ProteinGym (Notin et al.,
158 2024), tailored for protein fitness prediction and design. PEER (Xu et al., 2022), encompasses a
159 broad range of tasks including function prediction, localization, and structure analysis. However,
160 there is still a lack of benchmarks that comprehensively integrate multi-molecular tasks, which is
161 crucial for capturing the complex interactions between different moleculars in biological systems.
[Inspired by exciting multi-omics works and the lack of corresponding benchmarks, we present the](#)

Table 1: Overview of tasks of COMET across different molecule groups. Residue-level tasks require labels to have the same length as input nucleotide or amino acid sequences. Sequence-level tasks require one input sequence to share one label. Cls and Reg denote classification and regression.

Task	Omics	#Train/Val/Test	Metric	Task Type	Biology Level	Max/Mean Length/2	Source/Venue
DNA							
GE	DNA	16,413/1,000/1,000	R^2	Reg	Sequence	6,000/6,000	Xpresso/CR
EA	DNA	402,296/40,570/41,186	PCC	Multi-label Reg	Sequence	249/249	DeepStart/NM
RNA							
SSP	RNA	10,814/1,300/1,305	F1	Multi-label Cls	Residue	499/133.8	SPOT-RNA/NC
APA	RNA	145,463/33,170/49,755	R^2	Reg	Sequence	186/186	APARENT/Cell
PRS	RNA	73,227/9,153/9,154	R^2	Multi-label Reg	Sequence	148/148	Angenent-Mari's/NC
Protein							
Ther	Protein	5,056/639/1,336	SCC	Reg	Sequence	2,694/579.5	FLIP/NeurIPS
Cont	Protein	25,299/224/40	P@L	Multi-label Cls	Residue	4,914/226.5	Proteinnet/BMC Bio
EC	Protein	13,090/1,465/1,604	Fmax	Multi-label Cls	Sequence	751/270.2	DeepFRI/NMI
Cross-molecules CDS/Protein							
Flu	CDS/Protein	21464 / 5366 / 27217	SCC	Reg	Sequence	714/714	Sarkisyan's/Nature
EC	CDS/Protein	11105/1397/1458	Fmax	Multi-label Cls	Sequence	7,581/1,021.6	DeepFRI/NMI
Beta-Lact	CDS/Protein	9202 / 2322 / 1080	SCC	Reg	Sequence	858/858	Firnberg's/MBE
Multi-molecules							
EPI	DNA-DNA	149,328/18,666/18,667	MCC	Multi-class Cls	Sequence	2,000/2000	EPI-DLMH/BIB
siRNA	RNA-RNA	18,186/2,273/2,274	Mixed Score	Reg	Sequence	21/20.98	SAIS/TIANGHI
AAN	Protien-Protien	22,359/1,242/3,301	MCC	Multi-class Cls	Sequence	271/238.77	DeepAAI/NMI
RPI	RNA-Protien	14,994/1,666/4,164	MCC	Multi-class Cls	Sequence	3,999/1,834.7	NPInterv2.0/NAR
CRI-Off	RNA-DNA	14,223/2,032/4,064	SCC	Reg	Sequence	23/23	DeepCRISPR/GB
DPF	DNA-Protein	500/55/128	LDDT	Multi-label Reg	Residue	290/50.11	DeepPBS/NM

first benchmark that encompasses single-omics tasks, cross-omics tasks, and multi-omics tasks spanning DNA, RNA, and protein sequences.

3 BENCHMARK TASKS

The following sections provide detailed information for 17 diverse tasks, including data statistics, evaluation metrics, and data sources as shown in Table 1.

3.1 DNA TASK

Gene Expression (GE) predicts the expression levels of genes and transcription factors (TFs) across diverse tissues, recorded in target $y \in \mathbb{R}$. We extracted 1575 TF expression datasets from the GTEx database after filtering out non-expressed TFs, ensuring high-quality and tissue-specific expression profiles. Additionally, we integrated gene expression data from Xpresso (Agarwal & Shendure, 2020), covering 56 tissues, and grouped them into 11 functional and regional categories, enabling a comprehensive analysis of cross-tissue gene expression. This regression task aims to evaluate the model’s ability to predict gene and TF expression levels using the R^2 value as the evaluation metric. *Impact:* Gene expression is crucial for understanding transcriptional regulation and functional dynamics across the genome. Accurately predicting expression levels can elucidate the regulatory networks underlying different cellular states and tissue-specific functions, offering deeper insights into how genetic and environmental factors jointly influence gene expression and contribute to phenotypic variation and disease mechanisms.

Enhancer Activity Prediction (EA) is a regression task that predicts enhancer activity for two promoters associated with distinct developmental and housekeeping transcriptional programs directly from the DNA sequence. The enhancer activity dataset released in (de Almeida et al., 2022) comprises 484,052 DNA sequences, each 249 nucleotides in length, measured for their quantitative enhancer activity towards either a developmental or a housekeeping promoter by a continuous target variable $y \in \mathbb{R}$. We employ PCC as the metric.

Impact: Enhancers are essential genomic elements that regulate cell type-specific transcription of target genes, influencing animal development and physiology. Their ability to activate transcription outside their native contexts suggests that critical regulatory information resides within their DNA sequences. Mutations in enhancers can alter their function, leading to developmental defects and contributing to human diseases. Understanding enhancer activity is crucial for revealing the regulatory networks governing gene expression.

3.2 RNA TASK

APA Isoform Prediction (APA) predicts the polyA site strength for each variant, represented as target $y \in \mathbb{R}$. We filter 228k sequences from Bogard’s dataset (Bogard et al., 2019) containing over

3 million APA reporter gene data . This regression task evaluates the proportion of proximal APA isoforms with the performance metric being the R^2 value.

Impact: Alternative polyadenylation is a key regulatory mechanism that diversifies RNA transcripts and protein isoforms through 3' UTR processing. By influencing transcription termination and interacting with RNA splicing, APA modulates gene expression, impacting various cellular functions.

Programmable RNA Switches (PRS) are synthetic RNA molecules designed to regulate gene expression by responding to specific RNA sequences. Each switch exists in one of three activity states, ON, OFF, or ON/OFF, depending on the presence or absence of its trigger RNA sequence. The target $y \in \mathbb{R}^3$ represents the three activity states. The dataset (Angenent-Mari et al., 2020) includes 91,534 in vivo toehold switches, covering 23 viral genomes and 906 human transcription factors. The activity of these switches is measured using GFP signal intensity, which provides a quantitative readout of switch performance. The effectiveness of these switches is evaluated using the R^2 metric.

Impact: Programmable RNA switches provide precise control of gene expression and cellular functions, making them essential in synthetic biology for manipulating biological processes both in vitro and in vivo. These RNAs act as responsive elements to small molecules, proteins, or nucleic acids, allowing fine regulation of cellular behavior. Therapeutically, they promise to enable targeted treatments by detecting disease-specific signals and triggering precise cellular responses, contributing to novel approaches in precision medicine and synthetic biology.

Secondary Structure Prediction (SSP) identifies paired nucleotide regions in stems and unpaired nucleotide regions in loops, bulges and junctions within RNA molecules. In a RNA molecule with a length of l , The target matrix $y \in \mathbb{R}^{l \times l}$ indicates whether each nucleotide and other nucleotides form a base pair. We utilize the bpRNA-1m database (Danaee et al., 2018). The performance metric for this task is the F1 score.

Impact: Accurate secondary structure prediction is paramount for elucidating the intricate mechanisms underlying function and dynamics. By mapping these structures, researchers gain insights that advance genetic research and guide RNA-based therapeutic development, supporting innovations in precision medicine.

3.3 PROTEIN TASK

Thermostability Prediction (Ther) is a regression task that aims to predict the stability of proteins at high temperatures. From the Thermostability task of FLIP (Dallago et al., 2021), we apply the ‘Human-cell’ splits. We use the Spearman correlation coefficient (SCC) as the metric.

Impact: Protein thermostability prediction advances our understanding of protein functions and properties. In industrial enzyme applications, developing highly thermostable enzymes is essential for operating under harsh reaction conditions (Wu et al., 2023). Such predictions facilitate directed evolution and selection of proteins, which is of great significance for drug and vaccine discovery (Chen & Gong, 2022).

Enzyme Commission Number Prediction (EC) involves annotating protein sequences. The data is sourced from the EC benchmark established in DEEPFRI (Gligorijević et al., 2021). We collect the corresponding codon sequences for the dataset simultaneously. It retains over 90% of the original samples after filtering out anomalous data. We use Fmax as the metric.

Impact: Identifying enzymes and their catalytic reaction types is crucial for understanding enzyme functions. This can accelerate the discovery of new enzymatic activities and improve the functions of existing enzymes. In the field of drug discovery, it can assist in designing enzymes with specific catalytic activities, supporting the development of novel drugs and therapies (Chautard et al., 2009).

Contact Map Prediction (Cont) aims to forecast interactions between amino acid residues in a protein. Given a protein’s amino acids sequence, the target is to predict which residues are in close proximity in its three-dimensional structure. The data is sourced from the Proteinnet (AlQuraishi, 2019) and TAPE benchmark (Rao et al., 2019). We use P@L/5 as the metric.

Impact: Accurate contact map prediction has a significant impact on the field of structural biology (Vendruscolo et al., 1997). It helps identify protein-protein interactions, protein folding pathways, and design new proteins with desired properties. As a powerful tool, it bridges the gap between protein sequence and structure.

Fluorescence Prediction (Flu) evaluates the model’s ability to predict fluorescence values for higher-order mutated green fluorescent protein (avGFP) sequences. The original data comes from

Sarkisyan et al. (2016) and Xu et al. (2022), following the settings outlined in Boshar et al. (2024). It's a regression task and we use SCC as the metric.

Impact: Accurately predicting the fluorescence values of higher-order mutated avGFP is crucial for understanding protein function. It helps to elucidate the relationship between sequence variations and function, enhancing the understanding of evolutionary landscapes. This enables the design of novel fluorescent proteins with specific properties, applicable in broader scenarios within synthetic biology.

Beta-Lactamase Prediction (Beta-Lac) aims to explore the fitness landscape of all single-codon mutations in a gene. The labels indicate the ability of mutated genes to confer resistance to penicillin. The data is sourced from Firnberg et al. (2014), and the complete settings from Boshar et al. (2024) are adopted. We use SCC as the metric.

Impact: Accurately predicting the impact of mutations on enzyme activity aids in understanding evolutionary processes at the molecular level and the mechanisms of disease. By predicting mutation effects, the specific functional mechanisms of proteins can be revealed. This has broad applications in drug development, disease treatment, industrial production, and agricultural production.

3.4 MULTI-MOLECULAR TASK

Enhancer-Promoter Interaction Prediction (EPI) is a single-label classification task in genomics that aims to identify interactions between enhancers and promoters sequence, with the categorical label $y \in \{0, 1\}$. The dataset, sourced from EPI-DLMH (Min et al., 2021), comprises six cell lines—GM12878, HUVEC, HeLa-S3, IMR90, K562, and NHEK. We sample to balance true EPIs and non-EPIs. We use the Matthews Correlation Coefficient (MCC) as the metric.

Impact: Enhancers are regulatory elements that can significantly enhance the transcription of genes located at varying distances, while promoters are essential regions where transcription begins. Understanding these interactions is crucial for deciphering the complex regulatory networks that govern cellular functions and can provide insights into developmental biology and disease mechanisms.

siRNA Efficiency Prediction (siRNA) is a regression task that aims to predict the silencing efficiency of different siRNAs. By inputting artificially modified siRNA sequences the target mRNA sequence, the model can estimate how effectively each siRNA silences its corresponding mRNA. This is a regression task, and we use Mixed Score as the evaluation metric A.5.1. The data utilized in this research are from SAIS (SAIS, 2020).

Impact: RNA interference (RNAi) is a natural gene expression regulation mechanism that reduces target protein levels by inhibiting the expression of target genes, typically achieved through siRNAs (Setten et al., 2019). With the success of mRNA vaccines in COVID-19 prevention, there has been growing interest in the development of nucleic acid-based drugs. Predicting the silencing efficiency of chemically modified siRNA sequences under the RNAi mechanism is crucial, as this metric is directly linked to the actual therapeutic efficacy of the drug.

Antibody-Antigen Neutralizability Prediction (AAN) is used to assess whether there is an interaction between an antigen and an antibody, making it a single-label classification task with the categorical label $y \in \{0, 1\}$. The goal is to predict whether a given antibody can bind to a specific antigen based on their sequences. This task is based on the HIV data from CATNAP (Yoon et al., 2015) and DeepAAI (Zhang et al., 2022). We use MCC as the metric.

Impact: To demonstrate the neutralizing effects of most natural and synthetic antibodies against any antigen, time-consuming, labor-intensive, and costly wet lab experiments are typically required (Lee et al., 2007). However, with machine learning, we can represent the neutralizing response of antibodies (Ab) from the perspective of Ab-Ag neutralization effects, highlighting similarities in binding regions. This approach also helps to enable the recommendation of broad-spectrum antibodies that can target new viral variants.

RNA-Protein Interaction Prediction (RPI) aims to forecast whether a non-coding RNA (ncRNA) interacts with RNA-binding protein (RBP). The dataset is sourced from NPInterv2.0 (Yuan et al., 2014). Since the databases only provide positive samples, which are pairs of ncRNA and proteins that interact, we utilized a negative sample dataset generated by ncRPI-LGAT (Han & Zhang, 2023), where ncRNAs and proteins are randomly paired. We use MCC as the metric.

Impact: The interaction between ncRNAs and RBPs plays a crucial role in various important biological processes, such as gene expression, chromatin modification, and epigenetic regulation. However, identifying ncRNA-protein interactions through wet-lab experiments remains time-consuming and expensive. The development of computational approaches to predict these interactions can significantly reduce the need for labor-intensive experiments, offering a more efficient and cost-effective

Table 2: Detailed specifications of Omics language models analyzed in the study.

Model	Omics	Num Parameters (M)	Max Token length	Pre-trained Data	Tokenizer	Positional Embedding
DNABERT2	DNA	114.79	128	Multispecies DNA	BPE	ALiBi
NTv2	DNA	94.00	1,000	Multispecies DNA	Non-overlap 6mer	RoPE
RNA-FM	RNA	99.90	1,024	Multispecies ncRNA	Single	APE
BEACON-B	RNA	86.12	1,024	Human ncRNA	Single	ALiBi
ESM-1b	Protein	653.11	1,024	Multispecies Protein	Single	APE
ESM-2	Protein	149.17	1,024	Multispecies Protein	Single	RoPE
LucaOne	Multi-omics	1,596.31	1,280	Multispecies DNA-RNA-Protein	Single	RoPE
CaLM	CDS	85.70	1,024	Codon Sequence	Non-overlap 3-mer	RoPE

solution. This task is essential for understanding RNA-protein regulatory mechanisms and their roles in diverse biological processes.

CRISPR Off-Target Prediction (CRI-Off) involves predicting the likelihood and frequency of off-target effects by inputting both the sgRNA sequence and the corresponding off-target DNA sequences. The specificity of sgRNA is measured by a continuous target variable $y \in \mathbb{R}$, reflecting the frequency of off-target cleavage events. The dataset from DeepCRISPR (Chuai et al., 2018) used for evaluation includes approximately 160,000 potential off-target sites from 30 sgRNAs across various cell types. SCC is employed as the performance metric to assess the relationship between predicted and observed off-target effects.

Impact: Precision in off-target predictions is crucial for advancing CRISPR technology, as it minimizes unintended genetic modifications that could result in harmful effects. Accurate off-target analysis is essential for refining sgRNA designs, thereby improving both the safety and efficacy of CRISPR applications in clinical and research settings. By ensuring that sgRNAs specifically target the desired DNA sequences, scientists can reduce the risk of unwanted mutations, making CRISPR-based therapies and genetic modifications more reliable and effective.

DNA-Protein Folding Prediction (DPF) predict the 3D structure of DNA-protein complexes by inputting their respective sequences. The training data is sourced from experimentally determined structural files found in DeepPBS (Mitra et al., 2024), which provide verified DNA-protein interaction data. From these datasets, pairs of DNA and protein sequences are extracted, along with their spatial coordinates. These coordinates serve as the labels for model training, allowing the model to learn the spatial relationships in the DNA-protein complex. The local Distance Difference Test (LDDT) is used as the evaluation metric to assess the accuracy of the predicted structures compared to the experimentally determined ones.

Impact: Transcription factors are essential for regulating various biological processes, including gene expression and cellular functions (Spitz & Furlong, 2012). Predicting protein-DNA binding specificity is crucial for understanding gene regulation, as proteins interact with DNA target sites with varying degrees of specificity. However, predicting binding specificity across different protein families remains a significant challenge (Chiu et al., 2023). Artificial intelligence can help overcome this by utilizing structural information from protein-DNA complexes to generalize predictions, enabling more accurate forecasts across protein families.

4 MODELS

We consider two types of baseline models in our benchmarks, including naive supervised models and pre-trained omics language models. We list the details in the following part in Table 2.

Naive Supervised Models. We employ three widely-used sequence encoders: CNN, ResNet and LSTM following the setting of BEACON and TAPE.

Pre-trained Omics Language Models. We evaluated the performance of single-omics, multi-omics and cross-omics language models. For single-omics language models, we utilize DNABERT2 (Zhou et al., 2023), NTv2 (Dalla-Torre et al., 2023), RNA-FM (Chen et al., 2022), BEACON-B (Ren et al., 2024), ESM-1b (Rives et al., 2021) and ESM-2 (Lin et al., 2023) for DNA, RNA, protein, cross-molecule and multi-molecule tasks. These models vary significantly in size, ranging from 86M to 653M parameters, and are pre-trained on diverse data sources including multispecies DNA, multispecies ncRNA, human ncRNA and multispecies protein. For multi-omics language models, we employ LucaOne (He et al., 2024), which is composed of a total of 1.8 billion parameters and is pre-trained on Multispecies DNA-RNA-Protein data. For cross-omics language models, Calm (Outeiral & Deane, 2024) incorporates codon embeddings into the protein language model, thereby utilizing codon sequences as pre-trained data.

Table 3: Results of different models on single-molecular tasks.

Model/Task	GE	EA (Dev)	EA (Hk)	APA	PRS	SSP	Cont	Ther	EC
Metric	$R^2(\%)$	PCC(%)	PCC(%)	$R^2(\%)$	$R^2(\%)$	F1(%)	P@ L/5(%)	SCC(%)	Fmax(%)
Literature SOTAs									
Literature SOTA	Xpresso	DeepSTARR	DeepSTARR	APARENT	MLP-O	UFold	MSATrans	ESM-1v	SaProt-GearNet
	44.06	68.00	74.00	50.82	55.67	65.40	82.10	78.00	88.90
Naive Supervised Model									
CNN	34.52	66.08	74.29	50.93	45.20	49.95	5.54	55.86	53.65
ResNet	38.65	67.41	75.84	56.45	55.33	57.26	7.69	54.17	64.09
LSTM	41.34	68.93	77.02	67.03	56.54	58.61	6.07	58.90	55.58
Pretrained Omics Language Model									
DNABERT2	46.40	68.22	77.43	72.40	54.79	24.05	3.84	16.54	6.69
NTv2	48.42	66.20	76.51	68.75	55.27	39.76	27.72	60.19	48.08
RNA-FM	40.07	68.87	77.76	70.32	55.98	68.50	5.12	55.31	28.09
BEACON-B	36.32	66.05	76.31	70.59	54.67	64.18	2.72	60.76	48.84
ESM-1b	26.37	62.21	73.81	68.82	54.42	57.87	45.08	70.94	88.48
ESM-2	34.77	68.04	77.03	69.52	56.27	68.75	55.54	69.36	85.46
LucaOne	47.70	68.54	77.76	69.25	58.26	56.47	27.31	68.30	81.11
Pretrained Omics Language Model (Frozen)									
DNABERT2	13.82	39.44	41.75	40.48	19.99	13.51	11.24	60.94	47.36
NTv2	13.78	29.36	28.89	30.86	23.09	14.72	7.48	60.95	40.57
RNA-FM	37.15	36.31	37.86	32.88	20.05	64.43	2.07	56.80	29.93
BEACON-B	23.61	34.57	38.63	41.21	25.73	58.73	12.15	57.18	39.08
ESM-1b	28.97	51.71	63.31	53.11	52.29	31.25	39.09	69.83	88.17
ESM-2	28.99	43.27	54.73	27.38	35.51	44.08	43.34	63.02	77.80
LucaOne	41.48	46.86	51.44	40.11	38.95	56.86	3.84	66.33	73.65

5 RESULTS

5.1 TRAINING SETUPS

To facilitate a rigorous comparison, we conduct comprehensive fine-tuning on all BERT-based pre-trained language models, including DNABERT-2, NTv2, RNA-FM, BEACON-B, ESM-1b, ESM-2, LucaOne, and CaLM. While all models are fine-tuned using identical training hyperparameters, LucaOne is subjected to LoRA fine-tuning, whereas full-parameter fine-tuning is applied to the remaining models. For the simpler supervised models (CNN, ResNet, and LSTM), we initialize training from scratch with analogous training configurations. We use and search the learning rate from 1×10^{-6} to 5×10^{-3} and keep its batch size to 32. All experiments are conducted on NVIDIA A100 GPUs. Additional information is available in Appendix A.2

5.2 SINGLE-MOLECULAR BENCHMARK RESULTS

In Table 3, we report the benchmark results on single-molecular tasks, including literature SOTAs, naive supervised models and existing omics language models. Literature SOTAs include Xpresso (Agarwal & Shendure, 2020), DeepSTARR (de Almeida et al., 2022), APARENT (Bogard et al., 2019), MLP-O (Angenent-Mari et al., 2020), UFold (Fu et al., 2022), MSATrans (Rao et al., 2021), ESM-1v (Meier et al., 2021), SaProt-GearNet (Su et al., 2023).

Randomly initialized vocabulary embeddings show other omics knowledge learned during pre-training. By fine-tuning with only replacing vocabulary embeddings, the pre-trained models for each omics can achieve comparable results on most other omics tasks. This indicates that the omics knowledge learned during pre-training is not only stored in word embeddings, but also has a considerable proportion in the encoder, and can achieve rapid knowledge transfer of different omics through embedding replacement. And it can also help to explore commonalities and connections between different omics.

Protein models enhance predictive performance in DNA and RNA regulatory tasks. ESM-2 achieves results comparable to DNA or RNA models on DNA EA task and RNA APA, and PRS tasks. Notably, it even surpasses the current best model RNA-FM on the challenging SSP task. This indicates that protein models can enhance the performance of DNA or RNA regulatory prediction tasks, aiding biologists in exploring regulatory networks between proteins and regulatory elements. **This cross-omics adaptability underscores the potential for multi-omics models that integrate nucleotide, codon, and protein-specific features to achieve more comprehensive biological insights.**

DNA models demonstrate potential in protein and RNA Tasks due to DNA’s role in the central dogma’s origin. The DNA model NTv2 achieves results close to protein models on the protein Ther task. Both DNABERT2 and NTv2 also perform comparably to RNA models on RNA tasks such as APA and PRS. This suggests that DNA models have the potential to learn the properties and functions of protein and RNA models because the DNA sequences used in pre-training include regions responsible for transcribing RNA and translating proteins. **This cross-domain adaptability**

Table 4: Results of different models on cross-molecular tasks.

Model/Task	Beta-Lac	Flu	EC	Model/Task	Beta-Lac	Flu	EC
Metric	SCC(%)	SCC(%)	Fmax(%)	Metric	SCC(%)	SCC(%)	Fmax(%)
Codon Sequence (CDS)				Protein Sequence			
Naive Supervised Model							
CNN	47.66	65.67	18.22	CNN	79.31	67.01	54.28
ResNet	27.20	66.98	33.68	ResNet	82.45	67.66	60.49
LSTM	16.92	67.27	30.46	LSTM	78.51	67.82	54.41
Pretrained Omics				Language Model			
DNABERT2	60.64	67.40	30.62	ESM-1b	85.27	68.12	87.12
NTv2	63.34	67.52	37.12	ESM-2	89.10	68.09	85.30
RNA-FM	26.45	59.47	36.37	LucaOne	81.08	67.73	78.32
BEACON-B	60.02	67.43	41.74				
CaLM	86.56	67.53	48.91				
LucaOne	82.25	67.95	52.91				
Pretrained Omics Language Model (Frozen)							
DNABERT2	25.51	31.14	28.51	ESM-1b	59.96	52.20	87.32
NTv2	42.31	42.10	20.90	ESM-2	47.97	47.53	76.04
RNA-FM	9.33	27.58	11.97	LucaOne	29.97	30.70	20.19
BEACON-B	14.40	22.69	36.54				
CaLM	43.11	39.73	73.42				
LucaOne	49.14	50.03	34.06				

showcases the inherent connection between DNA, RNA, and protein representations and emphasizes the importance of designing models that leverage this central dogma framework.

Single-omics models achieve competitive performance in their respective tasks, especially tasks about structure. Protein models consistently secured the best performance across all protein tasks. Similarly, DNA and RNA models achieve either the top performance or perform comparably to the best models within their respective domains. Notably, in more challenging structural prediction tasks, such as RNA SSP and Protein Cont, RNA and protein models outperformed most other models by a considerable margin. This is indicative of their robust capability in capturing intricate molecular features, making them well-suited for complex structural prediction tasks. The tailored pretraining on omics-specific data plays a significant role in this success.

Language models outperform naive supervised models. Language models outperform the naive supervised models on three types of single-molecular tasks. This suggests that pre-training on large-scale unlabeled data does help to uncover the latent knowledge in biological data.

5.3 CROSS-MOLECULAR BENCHMARK RESULTS

In Table 4, we compare the performance of existing protein models and DNA/RNA/CDS models on amino acid sequences and their corresponding codon sequences (CDS).

CDS model demonstrates competitive performance on codon sequence data. Experimental comparisons indicate that protein-based models applied to amino acid sequences outperform CaLM applied to corresponding codon sequences. This superior performance may be attributed to ESM models being pre-trained on extensive unlabeled protein data, which include numerous mutated sequences. Consequently, the amount of pre-training data for ESM models is significantly larger than that for CaLM, which was pre-trained on codon sequences. But we observe that on Beta-Lac and Flu tasks, codon sequence-based methods achieved comparative performance, indicating potential in downstream tasks related to codon-specific information. This finding highlights the importance of considering codon-level biases and genomic context for downstream biological applications.

Nucleotide models have the potential to compare with the CDS model. DNA models that were not directly pre-trained on codon sequences can still achieve results close to CaLM on tasks like Flu. Moreover, the RNA model BEACON-B can achieve results on three tasks that are close to or even surpass those of DNA models. This demonstrates that nucleotide models have the potential to implicitly learn codon patterns, enabling them to capture codon-to-amino acid mappings even when not explicitly trained for tasks. This insight underlines the adaptability of nucleotide-based models and their potential to handle a broader range of biological tasks with cross-molecular relevance.

5.4 MULTI-MOLECULAR BENCHMARK RESULTS

In Table 5 and Table 6, we explore the combination of existing single-omics models and the multi-omics model and other models for the multi-molecular tasks. Literature SOTAs include EPI-DLMH (Min et al., 2021), DeepAAI (Zhang et al., 2022), ncrPI-LGAT (Han & Zhang, 2023) and DeepCRISPR (Chuai et al., 2018).

Table 5: Results of different models on homo-omics multi-molecules.

Model/Task	EPI	Model/Task	AAN	Model/Task	siRNA
Metric	MCC (%)	Metric	MCC (%)	Metric	Mixed Score (%)
Literature SOTA					
EPI-DLMH	53.59	DeepAAI	54.90	-	-
Naive Supervised Model					
CNN	25.04	CNN	39.08	CNN	56.41
ResNet	56.76	ResNet	45.79	ResNet	61.74
LSTM	58.47	LSTM	39.73	LSTM	48.69
Pretrained Omics Language Model					
DNABERT2+NTv2	57.68	ESM-1b+ESM-2	49.48	BEACON-B+RNA-FM	49.68
DNABERT2+DNABERT2	24.59	ESM-1b+ESM-1b	49.63	BEACON-B+BEACON-B	49.60
NTv2+DNABERT2	12.94	ESM-2+ESM-1b	49.36	RNA-FM+BEACON-B	49.65
NTv2+NTv2	23.54	ESM-2+ESM-2	49.83	RNA-FM+RNA-FM	49.21
LucaOne	61.29	LucaOne	47.49	LucaOne	62.33
Pretrained Omics Language Model (Frozen)					
DNABERT2+NTv2	11.67	ESM-1b+ESM-2	44.31	BEACON-B+RNA-FM	49.86
DNABERT2+DNABERT2	10.60	ESM-1b+ESM-1b	48.09	BEACON-B+BEACON-B	49.73
NTv2+DNABERT2	6.47	ESM-2+ESM-1b	42.80	RNA-FM+BEACON-B	50.05
NTv2+NTv2	13.06	ESM-2+ESM-2	39.42	RNA-FM+RNA-FM	49.48
LucaOne	15.16	LucaOne	25.55	LucaOne	50.13

Table 6: Results of different models on heter-omics multi-molecules.

Model/Task	RPI	Model/Task	CRI-Off	Model/Task	DPF
Metric	MCC (%)	Metric	SC (%)	Metric	LDLT (%)
Literature SOTA					
ncRPI-LGAT	93.20	DeepCRISPR	12.60	-	-
Naive Supervised Model					
CNN	86.25	CNN	10.86	CNN	34.64
ResNet	87.39	ResNet	8.90	ResNet	33.14
LSTM	87.83	LSTM	7.63	LSTM	32.09
Pretrained Omics Language Model					
ESM-1b+RNA-FM	87.41	RNA-FM+NTv2	11.74	NTv2+ESM-1b	41.14
ESM-2+RNA-FM	88.8	RNA-FM+DNABERT2	7.36	DNABERT2+ESM-1b	43.54
ESM-1b+BEACON-B	88.31	BEACON-B+NTv2	9.21	NTv2+ESM-2	43.54
ESM-2+BEACON-B	87.99	BEACON-B+DNABERT2	5.61	DNABERT2+ESM-2	46.35
LucaOne	88.94	LucaOne	11.69	LucaOne	39.76
Pretrained Omics Language Model (Frozen)					
ESM-1b+RNA-FM	83.96	RNA-FM+NTv2	5.89	NTv2+ESM-1b	40.59
ESM-2+RNA-FM	82.83	RNA-FM+DNABERT2	3.87	DNABERT2+ESM-1b	39.90
ESM-1b+BEACON-B	85.64	BEACON-B+NTv2	4.70	NTv2+ESM-2	42.53
ESM-2+BEACON-B	84.01	BEACON-B+DNABERT2	3.14	DNABERT2+ESM-2	43.39
LucaOne	77.90	LucaOne	8.42	LucaOne	32.65

Multi-omics model can perform better than single-molecular models. Without freezing the backbone, LucaOne performs exceptionally well on many tasks such as siRNA, EPI, and RPI. It surpasses both the combination of the two single-omics models and the naive supervised model, highlighting the effectiveness of multi-omics models trained on integrated datasets. This demonstrates that a unified multi-omics representation can capture cross-omics dependencies better than combining task-specific single-omics models, particularly when the backbone remains trainable.

Multi-molecular tasks still present significant challenges. In the AAN, RPI, and CRI-Off tasks, neither the approach of combining two single-omics models nor using the multi-omics model LucaOne outperforms SOTA methods. This indicates that while multi-omics models like LucaOne show promise, they struggle in tasks requiring highly specialized architectures or domain knowledge, suggesting the need for further architectural innovations and task-specific adaptations.

6 CONCLUSION

In this work, we present COMET, the first comprehensive multi-omics benchmark, which encompasses 17 diverse tasks spanning DNA, RNA, Protein, cross-molecule and multi-molecule study. COMET aims to address the critical gap in standardized evaluation for kinds of omics models in biology. We explore the connections between models from different omics across various tasks, gaining insights into tasks in one omic can benefit from models trained on another. We also find that multi-omics tasks still present certain challenges. These discoveries will inform the design of future biological language models, promoting interaction and understanding among different omics rather than studying each omic in isolation. However, the current benchmark involves relatively limited models and tasks, and some downstream tasks that require additional inputs are not yet aligned. In the future, we plan to further expand the models and tasks covered, closely follow developments in cross-omics and multi-omics research, and explore the potential connections between different omics data more thoroughly.

REFERENCES

- 540
541
542 Josh Abramson, Jonas Adler, Jack Dunger, Richard Evans, Tim Green, Alexander Pritzel, Olaf
543 Ronneberger, Lindsay Willmore, Andrew J Ballard, Joshua Bambrick, et al. Accurate structure
544 prediction of biomolecular interactions with alphafold 3. *Nature*, pp. 1–3, 2024.
- 545
546 Vikram Agarwal and Jay Shendure. Predicting mrna abundance directly from genomic sequence
547 using deep convolutional neural networks. *Cell reports*, 31(7), 2020.
- 548
549 Sunny Ahmar, Sumbul Saeed, Muhammad Hafeez Ullah Khan, Shahid Ullah Khan, Freddy Mora-
550 Poblete, Muhammad Kamran, Aroosha Faheem, Ambreen Maqsood, Muhammad Rauf, Saba
551 Saleem, et al. A revolution toward gene-editing technology and its application to crop improve-
552 ment. *International Journal of Molecular Sciences*, 21(16):5665, 2020.
- 553
554 Mohammed AlQuraishi. Proteinnet: a standardized data set for machine learning of protein struc-
555 ture. *BMC bioinformatics*, 20:1–10, 2019.
- 556
557 Nicolaas M Angenent-Mari, Alexander S Garruss, Luis R Soenksen, George Church, and James J
558 Collins. A deep learning approach to programmable rna switches. *Nature communications*, 11
559 (1):5057, 2020.
- 560
561 Manoj Bhasin, Hong Zhang, Ellis L Reinherz, and Pedro A Reche. Prediction of methylated cpgs
562 in dna sequences using a support vector machine. *FEBS letters*, 579(20):4302–4308, 2005.
- 563
564 Nicholas Bogard, Johannes Linder, Alexander B Rosenberg, and Georg Seelig. A deep neural
565 network for predicting and engineering alternative polyadenylation. *Cell*, 178(1):91–106, 2019.
- 566
567 Sam Boshar, Evan Trop, Bernardo P de Almeida, Liviu Copoiu, and Thomas Pierrot. Are genomic
568 language models all you need? exploring genomic language models on protein downstream tasks.
569 *Bioinformatics*, pp. btae529, 2024.
- 570
571 Jordan Chapman, Ahmed E Ismail, and Cerasela Zoica Dinu. Industrial applications of enzymes:
572 Recent advances, techniques, and outlooks. *Catalysts*, 8(6):238, 2018.
- 573
574 Emilie Chautard, Nicolas Thierry-Mieg, and Sylvie Ricard-Blum. Interaction networks: from pro-
575 tein functions to drug discovery. a review. *Pathologie Biologie*, 57(4):324–333, 2009.
- 576
577 Jiayang Chen, Zhihang Hu, Siqi Sun, Qingxiong Tan, Yixuan Wang, Qinze Yu, Licheng Zong, Liang
578 Hong, Jin Xiao, Tao Shen, et al. Interpretable rna foundation model from unannotated data for
579 highly accurate rna structure and function predictions. *arXiv preprint arXiv:2204.00300*, 2022.
- 580
581 Tianlong Chen and Chengyue Gong. Hotprotein: A novel framework for protein thermostability
582 prediction and editing. *NeurIPS 2022*, 2022.
- 583
584 Tsu-Pei Chiu, Satyanarayan Rao, and Remo Rohs. Physicochemical models of protein–dna binding
585 with standard and modified base pairs. *Proceedings of the National Academy of Sciences*, 120(4):
586 e2205796120, 2023.
- 587
588 Yanyi Chu, Dan Yu, Yupeng Li, Kaixuan Huang, Yue Shen, Le Cong, Jason Zhang, and Mengdi
589 Wang. A 5 utr language model for decoding untranslated regions of mrna and function predictions.
590 *Nature Machine Intelligence*, 6(4):449–460, 2024.
- 591
592 Guohui Chuai, Hanhui Ma, Jifang Yan, Ming Chen, Nanfang Hong, Dongyu Xue, Chi Zhou, Chenyu
593 Zhu, Ke Chen, Bin Duan, et al. Deepcrispr: optimized crispr guide rna design by deep learning.
Genome biology, 19:1–18, 2018.
- Francis Crick. Central dogma of molecular biology. *Nature*, 227(5258):561–563, 1970.
- Hugo Dalla-Torre, Liam Gonzalez, Javier Mendoza-Revilla, Nicolas Lopez Carranza, Adam Henryk
Grzywaczewski, Francesco Oteri, Christian Dallago, Evan Trop, Bernardo P de Almeida, Hassan
Sirelkhatim, et al. The nucleotide transformer: Building and evaluating robust foundation models
for human genomics. *BioRxiv*, pp. 2023–01, 2023.

- 594 Christian Dallago, Jody Mou, Kadina E Johnston, Bruce J Wittmann, Nicholas Bhattacharya,
595 Samuel Goldman, Ali Madani, and Kevin K Yang. Flip: Benchmark tasks in fitness landscape
596 inference for proteins. *bioRxiv*, pp. 2021–11, 2021.
597
- 598 Padideh Danaee, Mason Rouches, Michelle Wiley, Dezhong Deng, Liang Huang, and David Hen-
599 drix. bprna: large-scale automated annotation and analysis of rna secondary structure. *Nucleic
600 acids research*, 46(11):5381–5394, 2018.
601
- 602 Bernardo P de Almeida, Franziska Reiter, Michaela Pagani, and Alexander Stark. Deepstarr pre-
603 dicts enhancer activity from dna sequence and enables the de novo design of synthetic enhancers.
604 *Nature genetics*, 54(5):613–624, 2022.
- 605 Elad Firnberg, Jason W Labonte, Jeffrey J Gray, and Marc Ostermeier. A comprehensive, high-
606 resolution map of a gene’s fitness landscape. *Molecular biology and evolution*, 31(6):1581–1592,
607 2014.
608
- 609 Laiyi Fu, Yingxin Cao, Jie Wu, Qinke Peng, Qing Nie, and Xiaohui Xie. Ufold: fast and accurate
610 rna secondary structure prediction with deep learning. *Nucleic acids research*, 50(3):e14–e14,
611 2022.
- 612 Vladimir Gligorijević, P Douglas Renfrew, Tomasz Kosciolk, Julia Koehler Leman, Daniel Beren-
613 berg, Tommi Vatanen, Chris Chandler, Bryn C Taylor, Ian M Fisk, Hera Vlamakis, et al. Structure-
614 based protein function prediction using graph convolutional networks. *Nature communications*,
615 12(1):3168, 2021.
616
- 617 Katarína Grešová, Vlastimil Martinek, David Čechák, Petr Šimeček, and Panagiotis Alexiou. Ge-
618 nomic benchmarks: a collection of datasets for genomic sequence classification. *BMC Genomic
619 Data*, 24(1):25, 2023.
- 620 Yong Han and Shao-Wu Zhang. ncrpi-igat: Prediction of ncRNA-protein interactions with line graph
621 attention network framework. *Computational and Structural Biotechnology Journal*, 21:2286–
622 2295, 2023.
623
- 624 Tomas Hayes, Roshan Rao, Halil Akin, Nicholas J Sofroniew, Deniz Oktay, Zeming Lin, Robert
625 Verkuil, Vincent Q Tran, Jonathan Deaton, Marius Wiggert, et al. Simulating 500 million years
626 of evolution with a language model. *bioRxiv*, pp. 2024–07, 2024.
- 627 Yong He, Pan Fang, Yongtao Shan, Yuanfei Pan, Yanhong Wei, Yichang Chen, Yihao Chen, Yi Liu,
628 Zhenyu Zeng, Zhan Zhou, et al. Lucaone: Generalized biological foundation model with unified
629 nucleic acid and protein language. *bioRxiv*, pp. 2024–05, 2024.
630
- 631 Yanrong Ji, Zhihan Zhou, Han Liu, and Ramana V Davuluri. Dnabert: pre-trained bidirectional
632 encoder representations from transformers model for dna-language in genome. *Bioinformatics*,
633 37(15):2112–2120, 2021.
634
- 635 Chia Hsiang Kao, Evan Trop, McKinley Polen, Yair Schiff, Bernardo P de Almeida, Aaron
636 Gokaslan, Thomas Pierrot, and Volodymyr Kuleshov. Advancing dna language models: The
637 genomics long-range benchmark. In *ICLR 2024 Workshop on Machine Learning for Genomics
638 Explorations*, 2024.
- 639 Alexander Karollus, Žiga Avsec, and Julien Gagneur. Predicting mean ribosome load for 5’utr of
640 any length using deep learning. *PLoS computational biology*, 17(5):e1008982, 2021.
641
- 642 Charu Kathuria, Deepti Mehrotra, and Navnit Kumar Misra. Predicting the protein structure using
643 random forest approach. *Procedia computer science*, 132:1654–1662, 2018.
- 644 Duc-Hau Le. Machine learning-based approaches for disease gene prediction. *Briefings in functional
645 genomics*, 19(5-6):350–363, 2020.
646
- 647 Carol MY Lee, Niccolo Iorno, Frederic Sierro, and Daniel Christ. Selection of human antibody
fragments by phage display. *Nature protocols*, 2(11):3001–3008, 2007.

- 648 Zeming Lin, Halil Akin, Roshan Rao, Brian Hie, Zhongkai Zhu, Wenting Lu, Nikita Smetanin,
649 Robert Verkuil, Ori Kabeli, Yaniv Shmueli, et al. Evolutionary-scale prediction of atomic-level
650 protein structure with a language model. *Science*, 379(6637):1123–1130, 2023.
- 651 Weiguang Mao, Dennis Kostka, and Maria Chikina. Modeling enhancer-promoter interactions with
652 attention-based neural networks. *bioRxiv*, pp. 219667, 2017.
- 654 Frederikke Isa Marin, Felix Teufel, Marc Horlacher, Dennis Madsen, Dennis Pultz, Ole Winther,
655 and Wouter Boomsma. Bend: Benchmarking dna language models on biologically meaningful
656 tasks. In *The Twelfth International Conference on Learning Representations*, 2023.
- 657 Joshua Meier, Roshan Rao, Robert Verkuil, Jason Liu, Tom Sercu, and Alex Rives. Language
658 models enable zero-shot prediction of the effects of mutations on protein function. *Advances in*
659 *neural information processing systems*, 34:29287–29303, 2021.
- 661 Xiaoping Min, Congmin Ye, Xiangrong Liu, and Xiangxiang Zeng. Predicting enhancer-promoter
662 interactions by deep learning and matching heuristic. *Briefings in Bioinformatics*, 22(4):bbaa254,
663 2021.
- 664 Raktim Mitra, Jinsen Li, Jared M Sagendorf, Yibei Jiang, Ari S Cohen, Tsu-Pei Chiu, Cameron J
665 Glasscock, and Remo Rohs. Geometric deep learning of protein–dna binding specificity. *Nature*
666 *Methods*, pp. 1–10, 2024.
- 668 Eric Nguyen, Michael Poli, Marjan Faizi, Armin Thomas, Michael Wornow, Callum Birch-Sykes,
669 Stefano Massaroli, Aman Patel, Clayton Rabideau, Yoshua Bengio, et al. Hyenadna: Long-range
670 genomic sequence modeling at single nucleotide resolution. *Advances in neural information*
671 *processing systems*, 36, 2024.
- 672 Pascal Notin, Aaron Kollasch, Daniel Ritter, Lood Van Niekerk, Steffanie Paul, Han Spinner, Nathan
673 Rollins, Ada Shaw, Rose Orenbuch, Ruben Weitzman, et al. Proteingym: Large-scale benchmarks
674 for protein fitness prediction and design. *Advances in Neural Information Processing Systems*, 36,
675 2024.
- 676 Carlos Outeiral and Charlotte M Deane. Codon language embeddings provide strong signals for use
677 in protein engineering. *Nature Machine Intelligence*, 6(2):170–179, 2024.
- 679 Mangal Prakash, Artem Moskalev, Peter A DiMaggio, Steven Combs, Tommaso Mansi, Justin
680 Scheer, and Rui Liao. Bridging biomolecular modalities for knowledge transfer in bio-language
681 models. *bioRxiv*, pp. 2024–10, 2024.
- 682 Roshan Rao, Nicholas Bhattacharya, Neil Thomas, Yan Duan, Peter Chen, John Canny, Pieter
683 Abbeel, and Yun Song. Evaluating protein transfer learning with tape. *Advances in neural infor-*
684 *mation processing systems*, 32, 2019.
- 686 Roshan M Rao, Jason Liu, Robert Verkuil, Joshua Meier, John Canny, Pieter Abbeel, Tom Sercu,
687 and Alexander Rives. Msa transformer. In *International Conference on Machine Learning*, pp.
688 8844–8856. PMLR, 2021.
- 689 Partha Pratim Ray. Chatgpt: A comprehensive review on background, applications, key challenges,
690 bias, ethics, limitations and future scope. *Internet of Things and Cyber-Physical Systems*, 3:
691 121–154, 2023.
- 693 Matthew IJ Raybould, Aleksandr Kovaltsuk, Claire Marks, and Charlotte M Deane. Cov-abdab: the
694 coronavirus antibody database. *Bioinformatics*, 37(5):734–735, 2021.
- 695 Yuchen Ren, Zhiyuan Chen, Lifeng Qiao, Hongtai Jing, Yuchen Cai, Sheng Xu, Peng Ye, Xinzhu
696 Ma, Siqi Sun, Hongliang Yan, et al. Beacon: Benchmark for comprehensive rna tasks and lan-
697 guage models. *arXiv preprint arXiv:2406.10391*, 2024.
- 699 Alexander Rives, Joshua Meier, Tom Sercu, Siddharth Goyal, Zeming Lin, Jason Liu, Demi Guo,
700 Myle Ott, C Lawrence Zitnick, Jerry Ma, et al. Biological structure and function emerge from
701 scaling unsupervised learning to 250 million protein sequences. *Proceedings of the National*
Academy of Sciences, 118(15):e2016239118, 2021.

- 702 Frederic Runge, Karim Farid, Jorg KH Franke, and Frank Hutter. Rnabench: A comprehensive
703 library for in silico rna modelling. *bioRxiv*, pp. 2024–01, 2024.
704
- 705 SAIS. sirna data. [http://competition.sais.com.cn/competitionDetail/
706 532230/format](http://competition.sais.com.cn/competitionDetail/532230/format), 2020. Accessed: 2024-05-26.
- 707 Karen S Sarkisyan, Dmitry A Bolotin, Margarita V Meer, Dinara R Usmanova, Alexander S Mishin,
708 George V Sharonov, Dmitry N Ivankov, Nina G Bozhanova, Mikhail S Baranov, Onuralp Soyle-
709 mez, et al. Local fitness landscape of the green fluorescent protein. *Nature*, 533(7603):397–401,
710 2016.
711
- 712 Ryan L Setten, John J Rossi, and Si-ping Han. The current state and future directions of rna-based
713 therapeutics. *Nature reviews Drug discovery*, 18(6):421–446, 2019.
- 714 Dustin Shigaki, Orit Adato, Aashish N Adhikari, Shengcheng Dong, Alex Hawkins-Hooker, Fu-
715 mitaka Inoue, Tamar Juven-Gershon, Henry Kenlay, Beth Martin, Ayoti Patra, et al. Integration
716 of multiple epigenomic marks improves prediction of variant impact in saturation mutagenesis
717 reporter assay. *Human mutation*, 40(9):1280–1291, 2019.
718
- 719 Paweł Śledź and Amedeo Caflisch. Protein structure-based drug design: from docking to molecular
720 dynamics. *Current opinion in structural biology*, 48:93–102, 2018.
721
- 722 François Spitz and Eileen EM Furlong. Transcription factors: from enhancer binding to develop-
723 mental control. *Nature reviews genetics*, 13(9):613–626, 2012.
- 724 Jin Su, Chenchen Han, Yuyang Zhou, Junjie Shan, Xibin Zhou, and Fajie Yuan. Saprot: Protein
725 language modeling with structure-aware vocabulary. *bioRxiv*, pp. 2023–10, 2023.
726
- 727 Blake A Sweeney, Anton I Petrov, Carlos E Ribas, Robert D Finn, Alex Bateman, Maciej Szymanski,
728 Wojciech M Karlowski, Stefan E Seemann, Jan Gorodkin, Jamie J Cannone, et al. Rnacentral
729 2021: secondary structure integration, improved sequence search and new member databases.
730 *Nucleic Acids Research*, 49(D1), 2020.
- 731 Michele Vendruscolo, Edo Kussell, and Eytan Domany. Recovery of protein structure from contact
732 maps. *Folding and Design*, 2(5):295–306, 1997.
733
- 734 Hao Wu, Qiuming Chen, Wenli Zhang, and Wanmeng Mu. Overview of strategies for developing
735 high thermostability industrial enzymes: Discovery, mechanism, modification and challenges.
736 *Critical Reviews in Food Science and Nutrition*, 63(14):2057–2073, 2023.
- 737 Minghao Xu, Zuobai Zhang, Jiarui Lu, Zhaocheng Zhu, Yangtian Zhang, Ma Chang, Runcheng Liu,
738 and Jian Tang. Peer: a comprehensive and multi-task benchmark for protein sequence understand-
739 ing. *Advances in Neural Information Processing Systems*, 35:35156–35173, 2022.
740
- 741 Peng Ye, Weiqiang Bai, Yuchen Ren, Wenran Li, Lifeng Qiao, Chaoqi Liang, Linxiao Wang, Yuchen
742 Cai, Jianle Sun, Zejun Yang, et al. Genomics-fm: Universal foundation model for versatile and
743 data-efficient functional genomic analysis. *bioRxiv*, pp. 2024–07, 2024.
- 744 Hyejin Yoon, Jennifer Macke, Anthony P West Jr, Brian Foley, Pamela J Bjorkman, Bette Korber,
745 and Karina Yusim. Catnap: a tool to compile, analyze and tally neutralizing antibody panels.
746 *Nucleic acids research*, 43(W1):W213–W219, 2015.
747
- 748 Jiao Yuan, Wei Wu, Chaoyong Xie, Guoguang Zhao, Yi Zhao, and Runsheng Chen. Npinter v2. 0:
749 an updated database of ncna interactions. *Nucleic acids research*, 42(D1):D104–D108, 2014.
- 750 Jie Zhang, Yishan Du, Pengfei Zhou, Jinru Ding, Shuai Xia, Qian Wang, Feiyang Chen, Mu Zhou,
751 Xuemei Zhang, Weifeng Wang, et al. Predicting unseen antibodies’ neutralizability via adaptive
752 graph neural networks. *Nature Machine Intelligence*, 4(11):964–976, 2022.
753
- 754 Jiongmin Zhang, Man Zhu, and Ying Qian. protein2vec: predicting protein-protein interactions
755 based on lstm. *IEEE/ACM Transactions on Computational Biology and Bioinformatics*, 19(3):
1257–1266, 2020.

756 Zhihan Zhou, Yanrong Ji, Weijian Li, Pratik Dutta, Ramana Davuluri, and Han Liu. Dnabert-
757 2: Efficient foundation model and benchmark for multi-species genome. *arXiv preprint*
758 *arXiv:2306.15006*, 2023.

759 Xiao Zhu, Chenchen Qin, Fang Wang, Fan Yang, Bing He, Yu Zhao, and Jianhua Yao. Cd-gpt:
760 A biological foundation model bridging the gap between molecular sequences through central
761 dogma. *bioRxiv*, pp. 2024–06, 2024.

762
763 Zhong Zhuang, Xiaotong Shen, and Wei Pan. A simple convolutional neural network for prediction
764 of enhancer–promoter interactions with dna sequence data. *Bioinformatics*, 35(17):2899–2906,
765 2019.

766
767
768
769
770
771
772
773
774
775
776
777
778
779
780
781
782
783
784
785
786
787
788
789
790
791
792
793
794
795
796
797
798
799
800
801
802
803
804
805
806
807
808
809

A APPENDIX

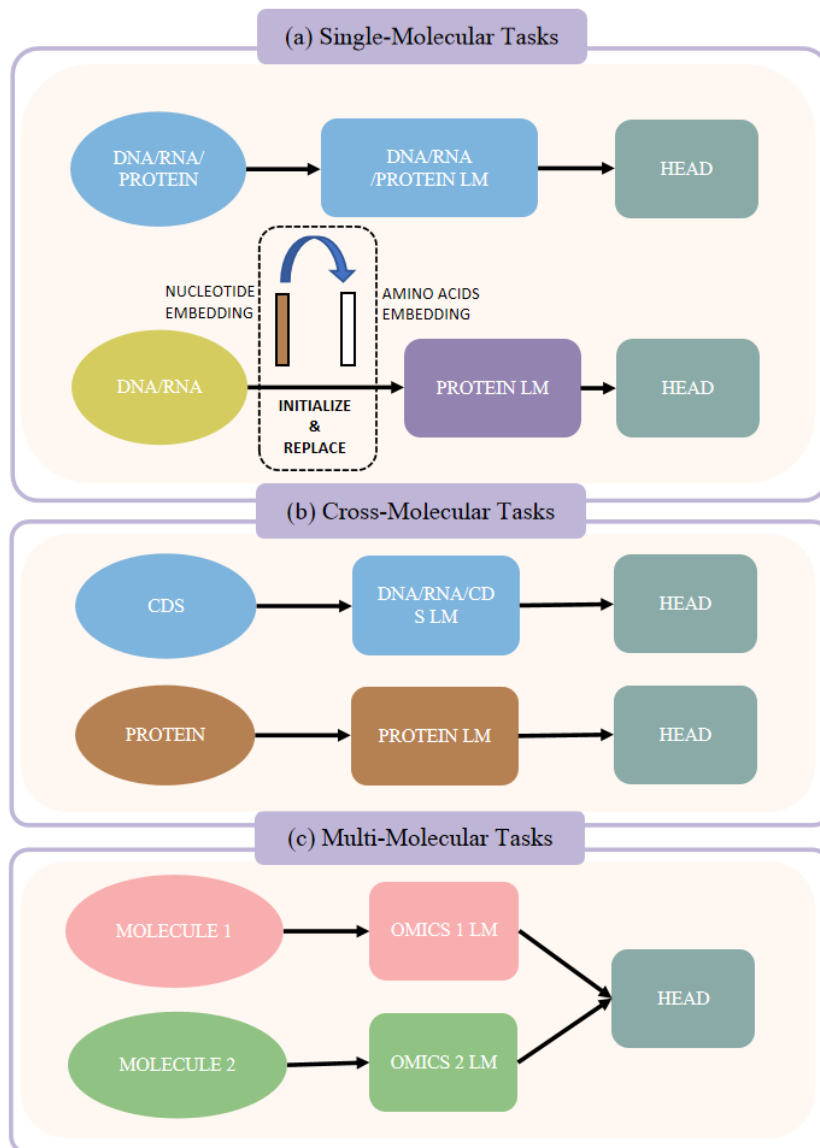


Figure 2: Detailed omics task pipeline of three kinds of tasks.

A.1 OMICS TASK PIPELINE

These are detailed pipelines conducted in experiments and shown in Figure 2.

Single-Molecular Task In single-molecule tasks, in addition to testing with models and tasks belonging to the same molecule, we also evaluate the performance of models and tasks across different molecules. To address the issue of inconsistent vocabularies, we reinitialized the vocab embeddings while loading the pretrained weights. For example, DNA/RNA models initialize and replace the nucleotide vocab embedding with initial amino acids vocab embedding when using protein data.

Cross-Molecular Task Cross-molecule tasks involve the corresponding protein sequences and codon sequences. Therefore, we first use open-source tools and datasets to collect and construct the CDS-Protein data. Subsequently, we can input CDS data for DNA/RNA/CDS models and input

protein data for protein models. Since Lucaone is a multi-omics model capable of processing both CDS and protein sequences, these inputs are handled separately.

Multi-Molecular Task In multi-molecule tasks, we use different omics models with different omics molecules. By rotating foundation models within single-omics, we achieved a unified evaluation of multi-omics data. For example, a DNA-DNA task can be processed by any combination of two models within the DNA foundation model.

A.2 BIOLOGY TASK PIPELINE

Sequence Level Prediction The architecture for sequence-level prediction tasks varies depending on whether the task involves single-molecule or multi-molecule scenarios.

For single-molecule sequence-level predictions, we utilize different strategies based on the model type. For naive supervised models, we compute an attentive weighted sum of all nucleotides to form a single sequence representation, which is then passed through an MLP to produce the final predictions. In contrast, when using language models, the [CLS] token representation is extracted and fed into a classifier layer to obtain the output predictions.

For multi-molecule sequence-level prediction tasks, the two interacting molecular sequences are processed independently using the same approaches as in the single-molecule scenario. Specifically, each molecule’s sequence is encoded separately using either a naive supervised model or a language model to generate individual representations. The resulting embeddings are then concatenated. In specific cases, such as sgRNA and CRI-Off, additional data features are incorporated along with the concatenated embeddings. This combined representation is passed through an MLP layer to generate the final sequence-level predictions.

Nucleotide Level Prediction To investigate the relationships between nucleotides, we calculate the self-outer product of the nucleotide representations, resulting in a matrix that captures the pairwise interactions among nucleotides. This interaction matrix is then processed through a simple ResNet architecture to produce the final output.

Amino Acids Level Prediction To study the relationships between residue pairs, we employed two approaches. For the transformer-based foundational language model, we extracted the attention matrix from the backbone encoder and appended a linear layer to directly predict the residue pair relationships. For the naive supervised model, we computed the feature matrix by calculating the point-wise product between token pairs, followed by a linear layer for relationship prediction.

A.2.1 MAX SEQUENCE LENGTH

Table 7 presents the maximum nucleotide and protein sequence lengths for tokenizers of each language model. Models such as DNABERT2, NTv2, and CaLM utilize relative positional encoding, providing excellent scalability to handle long sequences. Additionally, the BPE, non-overlap 6-mer, and non-overlap 3-mer tokenizer efficiently reduce the number of tokens, enabling these models to accommodate longer sequences under memory constraints. As a result, the maximum sequence lengths for DNABERT2, NTv2, and CaLM are set to 6000, 6002, and 3000, respectively. If a nucleotide or protein sequence exceeds the maximum length during tokenization, the tokenizer truncates the sequence to the specified limit, preserving the leftmost portion of the sequence.

Table 7: Max sequence length for tokenizers

Models	Max sequence length
DNABERT2	6000
NTv2	6002
RNA-FM	1024
BEACON-B	1024
ESM-1b	1024
ESM-2	1024
LucaOne	1280
CaLM	1024

918 A.3 EXPERIMENTAL SETTINGS FOR TASKS

919 A.3.1 DNA TASKS

920 DNA tasks, including Gene expression and enhancer activity prediction are trained using the settings
921 shown in Table 8.

922 Table 8: Configuration settings for DNA tasks

923 Config/Task	GE	EA
924 optimizer	AdamW	AdamW
925 optimizer epsilon	1.00E-08	1.00E-08
926 optimizer momentum	$\beta_1, \beta_2 = 0.9, 0.999$	$\beta_1, \beta_2 = 0.9, 0.999$
927 weight decay	0.01	0.01
928 learning rate sch.	linear decay	linear decay
929 learning rate	[1e-5,5e-3]	[1e-5,5e-3]
930 warmup steps	100	50
931 epochs	25	30
932 total batch size	32	32
933 dtype	float16	float16

934 A.3.2 RNA TASKS

935 APA isoform prediction and programmable RNA switches are trained using the settings shown in
936 Table 9. And secondary structure prediction is trained using the settings shown in Table 10.

937 Table 9: Configuration settings for APA isoform prediction and programmable RNA switches

938 Config/Task	APA	PRS
939 optimizer	AdamW	AdamW
940 optimizer epsilon	1.00E-08	1.00E-08
941 optimizer momentum	$\beta_1, \beta_2 = 0.9, 0.999$	$\beta_1, \beta_2 = 0.9, 0.999$
942 weight decay	0.01	0.01
943 learning rate sch.	linear decay	linear decay
944 learning rate	[1e-5,5e-3]	[1e-5,5e-3]
945 warmup steps	50	50
946 epochs	30	30
947 total batch size	32	32
948 dtype	float16	float16

949 Table 10: Configuration settings for secondary structure prediction

950 Config/Task	SSP
951 optimizer	Adam
952 optimizer epsilon	1e-08
953 optimizer momentum	$\beta_1, \beta_2 = 0.9, 0.999$
954 learning rate sch.	cosine decay
955 learning rate	[1e-5,5e-3]
956 warmup epochs	1
957 epochs	100
958 total batch size	32
959 dtype	float16

960 A.3.3 PROTEIN TASKS

961 All protein tasks, including thermostability prediction, enzyme commission number prediction and
962 contact map prediction are trained using the settings shown in Table 11.

972
973
974
975
976
977
978
979
980
981
982
983
984
985
986
987
988
989
990
991
992
993
994
995
996
997
998
999
1000
1001
1002
1003
1004
1005
1006
1007
1008
1009
1010
1011
1012
1013
1014
1015
1016
1017
1018
1019
1020
1021
1022
1023
1024
1025

Table 11: Configuration settings for protein tasks

Config/Task	Cont	Ther	EC
optimizer	AdamW	AdamW	AdamW
optimizer epsilon	1.00E-08	1.00E-08	1.00E-08
optimizer momentum	$\beta_1, \beta_2 = 0.9, 0.98$	$\beta_1, \beta_2 = 0.9, 0.98$	$\beta_1, \beta_2 = 0.9, 0.98$
weight decay	0.01	0.01	0.01
learning rate sch.	constant	constant	constant
learning rate	[2e-5, 1e-3]	[2e-5, 1e-3]	[2e-5, 1e-3]
epochs	50	200	100
total batch size	8	8	16
dtype	float16	float16	float16

A.3.4 CROSS-MOLECULER CDS/PROTEIN TASKS

In cross-molecule tasks, when the inputs are codon sequences, the settings used are shown in Table 12, while when the inputs are protein sequences, the settings used are shown in Table 13.

Table 12: Configuration settings for cross-molecules codon sequence inputs

Config/Task	Beta-Lac	Flu	EC
optimizer	AdamW	AdamW	AdamW
optimizer epsilon	1.00E-08	1.00E-08	1.00E-08
optimizer momentum	$\beta_1, \beta_2 = 0.9, 0.999$	$\beta_1, \beta_2 = 0.9, 0.999$	$\beta_1, \beta_2 = 0.9, 0.999$
weight decay	0.01	0.01	0.01
learning rate sch.	linear decay	linear decay	linear decay
learning rate	[1e-5, 5e-3]	[1e-5, 5e-3]	[1e-5, 5e-3]
warmup steps/epoch	100	100	50
epochs	100	100	100
total batch size	32	32	32
dtype	float16	float16	float16

Table 13: Configuration settings for cross-molecules protein sequence inputs

Config/Task	Beta-Lac	Flu	EC
optimizer	AdamW	AdamW	AdamW
optimizer epsilon	1.00E-08	1.00E-08	1.00E-08
optimizer momentum	$\beta_1, \beta_2 = 0.9, 0.98$	$\beta_1, \beta_2 = 0.9, 0.98$	$\beta_1, \beta_2 = 0.9, 0.98$
weight decay	0.01	0.01	0.01
learning rate sch.	constant	constant	constant
learning rate	[2e-5, 1e-3]	[2e-5, 1e-3]	[2e-5, 1e-3]
warmup steps/epoch	0	0	0
epochs	100	100	200
total batch size	64	64	16
dtype	float16	float16	float16

A.3.5 MULTI-MOLECULER TASKS

EPI, siRNA and AAN tasks are trained using the settings shown in Table 14. And RPI, CRI-Off tasks are trained using the settings shown in Table 15. The training settings of DPF are shown in Table 16.

1026
1027
1028
1029
1030
1031
1032
1033
1034
1035
1036
1037
1038
1039
1040
1041
1042
1043
1044
1045
1046
1047
1048
1049
1050
1051
1052
1053
1054
1055
1056
1057
1058
1059
1060
1061
1062
1063
1064
1065
1066
1067
1068
1069
1070
1071
1072
1073
1074
1075
1076
1077
1078
1079

Table 14: Configuration settings for EPI, siRNA and AAN

Config/Task	EPI	siRNA	AAN
optimizer	AdamW	AdamW	AdamW
optimizer epsilon	1.00E-08	1.00E-08	1.00E-08
optimizer momentum	$\beta_1, \beta_2 = 0.9, 0.999$	$\beta_1, \beta_2 = 0.9, 0.999$	$\beta_1, \beta_2 = 0.9, 0.999$
weight decay	0.01	0.01	0.01
learning rate sch.	constant	constant	constant
learning rate	[5e-6, 5e-5]	[5e-6, 5e-5]	[5e-6, 5e-5]
warmup steps	50	50	50
epochs	30	30	30
total batch size	64	64	32
dtype	float16	float16	float16

Table 15: Configuration settings for RPI and CRI-Off

Config/Task	RPI	CRI-Off
optimizer	AdamW	AdamW
optimizer epsilon	1.00E-08	1.00E-08
optimizer momentum	$\beta_1, \beta_2 = 0.9, 0.999$	$\beta_1, \beta_2 = 0.9, 0.999$
weight decay	0.01	0.01
learning rate sch.	constant	constant
learning rate	[5e-6, 5e-5]	[5e-6, 5e-5]
warmup steps/epoch	50	50
epochs	30	30
total batch size	64	32
dtype	float16	float16

Table 16: Configuration settings for Dna-Protein Folding

Config/Task	DPF
optimizer	AdamW
optimizer epsilon	1.00E-08
optimizer momentum	$\beta_1, \beta_2 = 0.9, 0.999$
weight decay	0.05
learning rate sch.	cosine decay
learning rate for DNA or protein model	[0,3e-5]
learning rate for ResNet and diffusion model	[0,1e-4]
warmup ratio	10%
epochs	100
batch size for DNA or protein model	1
batch size for ResNet and diffusion model	1
dtype	float16

A.4 DETAILED DATA PREPROCESSING FOR EACH TASK

A.4.1 GENE EXPRESSION

We adopt the data processing methodology from Xpresso (Agarwal & Shendure, 2020). Human gene expression data comes from the Epigenomics Roadmap Consortium, which provides normalized RNA-seq values for protein-coding mRNAs across 56 tissues and cell lines.

Due to the large number of parameters in biological language models and the memory limitations of A100 GPUs, our experiments show that trimming sequence lengths to 6000 bp ensures compatibility with all models for processing input sequences. By inputting consecutive 6000 bp nucleotide fragments from different positions in the processed sequences into the Xpresso model, we identify that the sequence indexed from position 7000 to 12999 (length 6000 bp) achieves optimal test performance. This segment contains the most information related to gene expression levels.

For training, we use the 6000 bp nucleotide sequence indexed from position 7000 to 12999 as input and the expression data for 56 tissues as labels. The train, validation, and test dataset splits follow the methodology used in Xpresso.

A.4.2 ENHANCER ACTIVITY PREDICTION

We follow the processing procedure described in (de Almeida et al., 2022). The data includes sequence information and transcriptional activity metrics for both *Drosophila* and humans, encompassing developmental and housekeeping transcriptional activity levels.

We use downloaded sequences of 249 bp in length, along with `Dev_log2_enrichment_scaled` and `Hk_log2_enrichment_scaled`, which respectively represent developmental and housekeeping transcriptional activity information. The dataset is divided into training, validation, and test sets according to the method outlined in (de Almeida et al., 2022).

A.4.3 APA ISOFORM PREDICTION

The preparation for IPA isoform analysis begins by filtering raw sequencing reads from all MPRA (Shigaki et al., 2019) to retain only high-quality, full-length RNA sequences. These reads are grouped based on the randomized regions located upstream of the proximal polyadenylation site (pPAS), forming a dictionary of sequence variants for each library. To expand this dictionary, sequencing is also performed on the plasmid library, capturing members that lack expression of a distal isoform. RNA reads are then matched to dictionary entries by identifying the upstream region with the shortest Hamming distance.

Polyadenylation cleavage sites are determined for each mapped read by detecting the presence of a Poly-A tail. The cleavage positions are recorded as vectors associated with individual sequence variants, including a specific position for reads mapping to non-random distal sites. The dataset generated from this process consists of a dictionary of distinct sequence variants paired with vectors of cleavage position counts. A final filtering step ensures data quality by discarding sequences supported by fewer than 10–20 unique UMI RNA reads or those containing over 75% A-nucleotides within a 12–20 bp region, which could indicate internal priming artifacts.

We process data from 12 random 3' UTR libraries. 9 among the 12 libraries are used for training and 3 held out (the 3 held-out libraries were excluded from the current analysis). To construct a balanced test set, sequences from each library are first shuffled independently according to their read counts. These shuffled sequences are then merged using a round-robin approach, selecting one sequence from each library at a time in descending order of read count. This strategy ensures that the test set contains an even representation of high-read count sequences across all libraries. The remaining sequences are appended to the beginning of the combined library, and the training set is further shuffled to enhance randomness. For benchmarking purposes, the top 10% of high-read count sequences are prioritized. Among these, the most abundantly expressed sequences are selected for testing, ensuring a high-quality, balanced dataset for training, validation, and evaluation.

1134 A.4.4 PROGRAMMABLE RNA SWITCHES

1135

1136 We adopt the data generation pipeline described in (Angenent-Mari et al., 2020). A toehold-switch
1137 library comprising 244,000 potential trigger sequences is designed and synthesized, covering the
1138 complete genomes of 23 pathogenic viruses, the entire coding regions of 906 human transcription
1139 factors, and approximately 10,000 random sequences. Using this synthesized oligo pool, two con-
1140 struct libraries are created to represent the ON and OFF states, and both are transformed into BL21
1141 E. coli. The OFF library includes toehold-switch constructs without triggers, while the ON library
1142 contains identical toeholds paired with complementary triggers fused to their respective switches.

1143 The libraries are sorted into four bins using fluorescence-activated cell sorting (FACS), and the
1144 variants in each bin are quantified through next-generation sequencing (NGS) to determine their
1145 fluorescence distributions. After quality control, the toehold-switch library consists of 109,067 ON-
1146 state measurements, 163,967 OFF-state measurements, and 91,534 ON/OFF paired ratios, where
1147 both states are characterized for each switch. ON and OFF data are normalized to a scale of 0 to
1148 1, with ON/OFF ratios normalized to a range of -1 to 1. Following (Angenent-Mari et al., 2020),
1149 a stringent quality control process is applied to eliminate artifacts and ensure data reliability. The
1150 quality control (QC) framework includes five levels: QC1, QC2, QC3, QC4 and QC5, where QC1
1151 represents the lowest quality and QC5 the highest. Datasets above QC2 are utilized for training,
1152 while QC5 is reserved for testing.

1153

1154 A.4.5 SECONDARY STRUCTURE PREDICTION

1155

1156 We follow the preprocessing steps outlined in the bpRNA-1m dataset (Danaee et al., 2018). To re-
1157 duce sequence redundancy and improve dataset diversity, we implement an 80% sequence-identity
1158 threshold and cap the maximum sequence length at 500 nucleotides, following protocols described
1159 in the referenced studies. These measures are essential for minimizing overfitting and ensuring that
1160 the models are trained on a wide range of genetically diverse samples.

1161 The dataset is divided into three subsets: a training set (TR0), a validation set (VL0), and a test
1162 set (TS0). The splitting process is randomized to eliminate potential biases and ensure an unbiased
1163 evaluation of the model’s performance.

1164

1165 A.4.6 PROTEIN TASKS

1166

1167 We obtain data of thermostability prediction, enzyme commission number prediction and contact
1168 map prediction from Saprot (Su et al., 2023). Following the guidance on github, we download data
1169 and place in the LMDB folder for supervised fine-tuning.

1170

1171 A.4.7 CROSS-MOLECULER TASKS

1172

1173 For the enzyme commission number prediction task, to obtain the codon information corresponding
1174 to protein sequences, we use UniProtKB mapping function to convert UniProt IDs into European
1175 Nucleotide Archive entries. We then employ the Smith-Waterman algorithm to quickly match the
1176 corresponding codon sequences, filtering out all sequences that contained unknown nucleotides or
1177 where the number of matched nucleotides is not a multiple of three. For other cross-omics tasks, we
1178 adopt the data and settings from (Boshar et al., 2024).

1179

1180 A.4.8 ENHANCER-PROMOTER INTERACTION PREDICTION

1181

1182 We follow the processing of (Min et al., 2021). We derive dataset from EPIANN (Mao et al., 2017),
1183 which includes six cell lines, GM12878, HeLa-S3, IMR90, K562, HUVEC and NHEK. To address
1184 the challenge of data imbalance, EPIANN enhanced the representation of positive samples by incor-
1185 porating the upstream and downstream regions of enhancers. This approach expanded the dataset to
1186 include relevant genomic regions by defining extended windows of 3 kbp around enhancers and 2
1187 kbp around promoters, ensuring a more comprehensive capture of the surrounding regulatory land-
scape.

1188 A.4.9 siRNA EFFICIENCY PREDICTION

1189 We get the dataset from SAIS (SAIS, 2020). We use the information of the reference sequence of the target gene, the sense sequence of the target gene, the sense sequence of modified siRNA and the remaining percentage of mRNA after the experiment named `gene_target_seq`, `siRNA_sense_seq`, `modified_siRNA_sense_seq` and `mRNA_remaining_pct` in dataset from SAIS, respectively.

1196 A.4.10 ANTIBODY-ANTIGEN NEUTRALIZABILITY PREDICTION

1197 We follow (Zhang et al., 2022), which provides a minimal dataset specifically designed for this prediction task. This task is based on two datasets: CATNAP (Yoon et al., 2015), which focuses on HIV, and CoVAbDab (Raybould et al., 2021), which pertains to SARS-CoV-2.

1201 HIV data is sourced from CATNAP in the Los Alamos HIV Database. Antibody (Ab) and antigen (Ag) sequences are extracted, curated to remove duplicates and missing values, and classified as neutralizing ($IC_{50} < 10 \mu\text{g/ml}$) or non-neutralizing ($IC_{50} \geq 10 \mu\text{g/ml}$). Seen and unseen Abs are split, ensuring no overlap between training, validation, and testing sets by excluding similar pairs (BlastP $\geq 90\%$). Training is conducted on seen Abs, with unseen Abs used for evaluation across 20 random dataset splits.

1207 SARS-CoV-2 Data is collected from CoVAbDab and includes pairwise Ab–Ag instances across variants like Alpha, Beta, Delta, and Omicron. Five sequences per variant and 11 for Omicron are used. Omicron is treated as an unseen Ag, excluded from training but incorporated in relation graphs for transductive learning, enabling the identification of broad-spectrum Abs.

1212 A.4.11 RNA-PROTEIN INTERACTION PREDICTION

1213 The dataset is sourced from NPInter2.0 , NPInter2.0.lncRNA , and RPI7317 . The sequences of ncRNAs and proteins are obtained from the NONCODE database , Gencode database , and UniProt database . The NPInter database integrates new datasets from literature and related resources, with a major focus on data published in recent years. Through a systematic PubMed search using keywords related to RNA interactions, 1270 relevant articles were identified. Verified or processed interaction data were manually extracted, while raw sequencing data were excluded. Binding sites were compared against RefSeq coding genes to remove overlaps with coding regions and cross-checked with NONCODE for ncRNA references. Valid interactions were annotated with standardized IDs (UniProt, RefSeq, NONCODE, etc.) depending on the molecule type.

1222 Data from external resources like LncRNADisease, which curated 478 experimentally supported lncRNA interactions, were integrated and subjected to the same annotation pipeline. The combined dataset underwent redundancy elimination, aggregating overlapping interactions into single records. NPInter v2.0 thus provides a comprehensive, curated multilevel snapshot of RNA-related interactions.

1228 A.4.12 CRISPR OFF-TARGET PREDICTION

1229 Following (Chuai et al., 2018), we get the off-target dataset, which comprises two different cell types contains 30 sgRNAs. For all 30 sgRNAs, approximately 160,000 possible off-target sites across the entire genome are obtained. Off-target sites are annotated and standardized using the targeting cutting frequency (indel frequency) detected by different off-target detection methods.

1234 A.4.13 DNA-PROTEIN FOLDING PREDICTION

1236 We query the PDB database using the filenames provided by deepPBD (Mitra et al., 2024) to obtain the mmCIF files of DNA-protein complexes and get 428 mmCIF files. From the mmCIF files, we extract the coordinates, sequences, and certain bonding information of both DNA and proteins. When encountering modified residues or nucleotides in the mmCIF files, we follow the AlphaFold3 (Abramson et al., 2024) and map these residues or nucleotides to standard amino acids or DNA sequences using SCOP. We set the DNA-protein interface distance threshold to 5 Å. Based on this threshold, we derive the DNA-protein interface information. Subsequently, we match the

DNA and protein duplex information using the DNA-protein interface and sequence information. Finally, we obtained 683 DNA-protein complexes.

A.5 MULTI-MOLECULER TASKS

A.5.1 siRNA EFFICIENCY PREDICTION

We use siRNA modification features combined with sequence features to enhance mRNA target specificity.

For the metric, we use mixed score as the metric—a custom metric balances regression error and classification accuracy by integrating F1 score (harmonic mean of precision and recall), Mean Absolute Error (MAE), and Range-MAE (MAE computed within a range threshold) (SAIS, 2020).

The formula for Range-MAE is:

$$Range-MAE = \frac{1}{m} \sum_{i=1}^m |y_i - \hat{y}_i|,$$

where m is the number of samples with predicted values within the range $[0, 30]$. The Range-MAE evaluates the average absolute error of predictions in this specific range, with values in $[0, 100]$.

F1 combines precision and recall to evaluate the classification performance of predictions within the Remaining range, focusing on $[0, 30]$. It outputs a final F1 score between $[0, 1]$.

The mixed score will be calculated based on the following formula:

$$Mixed - score = 50\% \times \left(1 - \frac{MAE}{100}\right) + 50\% \times F1 \times \left(1 - \frac{Range-MAE}{100}\right)$$

The first part of the score formula focuses on the overall accuracy of the model, while the second part emphasizes prediction precision within the low Remaining range.

A.5.2 CRISPR OFF-TARGET PREDICTION

We use epigenetic features including CTCF, Dnase, H3K4me3 and RRBs combined with sequence features to enhance CRISPR target specificity.

A.5.3 DNA-PROTEIN FOLDING

The model architecture for Dna-Protein Folding task imitates AlphaFold3. We engage DNA and protein models as input embedders to get DNA and protein representations, respectively. The DNA and protein representations are transformed to form DNA-protein single representations and DNA-protein single representations, and fed into a ResNet to get the final DNA-protein single and pair representations. The diffusion module processes the final DNA-protein single and pair representations to generate the structure of DNA-protein complexes.

Differ from AlphaFold3, we replace the template module, the MSA module and the pairformer module with a ResNet architecture composed of eight residual blocks. Furthermore, we modify the original diffusion module to consist of two encoder blocks, two decoder blocks, and four diffusion transformer blocks. The losses consist of diffusion loss and distogram loss:

$$\mathcal{L}_{\text{loss}} = \alpha_{\text{diffusion}} \cdot \mathcal{L}_{\text{diffusion}} + \alpha_{\text{distogram}} \cdot \mathcal{L}_{\text{distogram}}$$

where $\alpha_{\text{diffusion}} = 4.0$ and $\alpha_{\text{distogram}} = 0.03$. Each item in the losses is followed to AlphaFold3.

A.6 METHODS IN BENCHMARK

All pre-trained biology foundation models utilize a Masked Language Modeling (MLM) objective.

For the MLM task, an input sequence is given, where 15% of its elements are randomly masked. The model processes this masked sequence and aims to predict the original elements. This strategy mirrors the Cloze test found in conventional language modeling.

- 1296 • 15% of the tokens in the sequence are masked.
- 1297
- 1298 • In 80% of the cases, the masked tokens are replaced by a special MASK token.
- 1299
- 1300 • In 10% of the cases, the masked tokens are substituted with a random token different from
- 1301 the original.
- 1302 • In the remaining 10% of cases, the masked tokens remain unchanged.

1303 A.6.1 DNABERT2

1304 **Training Data** DNABERT2 utilized datasets from the human genome and multiple species
1305 genomes, totaling 35.24 billion nucleotide bases. The human genome dataset comprised 2.75 billion
1306 nucleotide bases, while the multi-species genome dataset included 32.49 billion nucleotide bases
1307 from the genomes of 135 different species. During the data processing, all sequences containing 'N'
1308 were removed, leaving only those composed of ATCG nucleotides.

1309 A.6.2 NTV2

1310 **Training Data** NTV2 leverages three datasets: the Human reference genome dataset, which con-
1311 tains 3.2 billion nucleotides; the 1000 Genomes Project (1000G) dataset, featuring over 20.5 trillion
1312 nucleotides; and the Multispecies dataset, comprising 174 billion nucleotides from 850 species.

1313 During the preprocessing phase, all nucleotides outside of ATCG are replaced with 'N'. For both
1314 the multispecies and human reference datasets, the genomes are segmented into overlapping chunks
1315 of 6,100 nucleotides. Each chunk overlaps with the previous one by sharing the first 50 nucleotides
1316 and with the next one by sharing the last 50 nucleotides.

1317 A.6.3 RNA-FM

1318 **Training Data** The RNA-FM model is pre-training utilizing data sourced from RNACentral. To
1319 ensure the non-redundancy of the dataset, RNA-FM employs CD-HIT (specifically, CD-HIT-EST)
1320 with a threshold set at 100% sequence identity. This process led to a final dataset comprising 23.7
1321 million distinct RNA sequences.

1322 A.6.4 BEACON-B

1323 **Training Data** The BEACON-B model uses 523,934 human ncRNA sequences filtered from the
1324 total ncRNA in the RNACentral database Sweeney et al. (2020) as pre-training data.

1325 A.6.5 ESM1B

1326 **Training Data** The ESM-1b model was pre-trained on Uniref50, which comprises approximately
1327 30 million protein sequences. During the training process, sequences exceeding 1023 tokens (ex-
1328 cluding the CLS token) are randomly truncated to a length of 1023 tokens.

1329 A.6.6 ESM2

1330 **Training Data** The ESM-2 model is trained using the UniRef50 dataset. To enhance the data
1331 volume and diversity, during each training update, a mini-batch of sequences from UniRef50 is
1332 sampled and replaced with sequences uniformly sampled from the corresponding UniRef90 clusters.
1333 This approach allows the ESM-2 model to be trained on over 60 million protein sequences.

1334 A.6.7 CALM

1335 **Training Data** The CaLM model is pre-trained using cDNA data collected from the European
1336 Nucleotide Archive database. During preprocessing, sequences containing unknown nucleotides,
1337 start codons that are not ATG, internal stop codons, or a nucleotide count not divisible by three are
1338 removed. The final dataset consists of about 9 million cDNA sequences.

1350 A.6.8 PROS AND CONS ANALYSIS

1351
1352 We can see that all models are trained using MLM, among which the NTV2 model uses much more
1353 pre-training data than other models, which may make it more generalizable on more tasks. The
1354 RNA-based models are all pre-trained only on ncRNA, and BEACON-B only uses a small part of
1355 the pre-training data, which may affect their potential performance. Models like the protein-based
1356 model and the Calm codon model use amino acid (non-overlapping 3mer) encoding, which may
1357 have an advantage in tasks that focus on amino acid expression. For the RNA-FM and ESM-1b
1358 models, the use of absolute position encoding limits the length of their input sequences, which may
1359 affect their performance on long sequence tasks.

1360 A.7 LORA FINE-TUNING SETTINGS

1361
1362 We utilized LoRA fine-tuning to optimize LucaOne. The configuration settings for LoRA fine-
1363 tuning are presented in Table 17.

1364
1365 Table 17: Configuration settings of LoRA fine-tuning for LucaOne

1366 Config	1367 Value
1368 Weight Type	W_q, W_k, W_v, W_o
1369 LoRA rank	$r_q = r_k = r_v = r_o = 32$
1370 LoRA α	32
1371 Dropout Prob	0.05

1372 A.8 FURTHER DISCUSSION

1373
1374 We appreciate the reviewer’s suggestion and agree that future directions are crucial for expanding
1375 the impact of this work. We propose three potential areas for further exploration:

- 1376
1377 • Incorporating Additional Omics Data and Biological Priors: Expanding the benchmark to
1378 include additional omics data types and features that indirectly influence biological pro-
1379 cesses in downstream tasks will enhance its comprehensiveness. Integrating biological
1380 priors, such as pathway-level annotations, protein-protein interactions, or chromatin acces-
1381 sibility maps, can provide a more holistic view of molecular interactions and improve the
1382 relevance of downstream predictions.
- 1383 • Refining the Evaluation Pipeline for Multimodal Data: Developing a more sophisticated
1384 evaluation pipeline that better infuses multimodal data will be essential. For instance, met-
1385 rics that capture cross-modality consistency and assess how well models leverage com-
1386plementary information from multiple omics types can provide deeper insights into model
1387 performance. Additionally, incorporating metrics that account for the stochasticity and
1388 uncertainty inherent in biological systems can improve evaluation robustness.
- 1389 • Developing Novel Multi-Omics Foundation Models: Leveraging the insights gained from
1390 this benchmark, we aim to explore novel model architectures tailored for multi-omics data.
1391 These models could employ advanced techniques like attention-based integration and hi-
1392erarchical representations of omics modalities. The benchmarking insights will guide the
1393 design of these models, ensuring they address the specific challenges and opportunities
1394 identified in multi-omics tasks.

1395 These future directions aim to expand the scope and utility of the benchmark, driving the devel-
1396 opment of innovative methods and fostering deeper biological insights through more accurate and
1397 comprehensive modeling of multi-omics data.

1398 A.9 ASSETS

1400 A.9.1 SOFTWARE AND LIBRARIES

1401 The open-source software, and corresponding licenses are presented in Table 18. The data, licenses
1402 and corresponding URL are presented in Tab. 19
1403 Table 20.

1404
1405
1406
1407
1408
1409
1410
1411
1412
1413
1414
1415
1416
1417
1418
1419
1420
1421
1422
1423
1424
1425
1426
1427
1428
1429
1430
1431
1432
1433
1434
1435
1436
1437
1438
1439
1440
1441
1442
1443
1444
1445
1446
1447
1448
1449
1450
1451
1452
1453
1454
1455
1456
1457

Table 18: Software used in this work

Asset	License
FlashAttention	BSD-3-Clause
Pytorch	BSD-3-Clause
Pytorch Lightning	Apache-2.0
Huggingface	Apache-2.0
Scikit-Learn	BSD-3-Clause
Numpy	BSD-3-Clause
Matplotlib	Matplotlib License
Seaborn	Apache-2.0

1458
1459
1460
1461
1462
1463
1464
1465
1466
1467
1468
1469
1470
1471
1472
1473
1474
1475
1476
1477
1478
1479
1480
1481
1482
1483
1484
1485
1486
1487
1488
1489
1490
1491
1492
1493
1494
1495
1496
1497
1498
1499
1500
1501
1502
1503
1504
1505
1506
1507
1508
1509
1510
1511

Table 19: Dataset used in this work(Part 1)

Dataset	Sub-dataset	License	URL
Enhancer Activity	Deepstarr	MIT	https://zenodo.org/records/5502060
Gene Expression	Xpresso	MIT	https://xpresso.gs.washington.edu
	GTE _x		https://www.gtexportal.org/home/
APA Isoform	APARENT	MIT	shttps://github.com/johli/aparent
Programmable RNA Switches	GEO	MIT	https://www.ncbi.nlm.nih.gov/geo/query/acc.cgi?acc=GSE149225
Secondary Structure			https://bprna.cgrb.oregonstate.edu/about.php
	CRW		https://crw-site.chemistry.gatech.edu
	tmRDB	Research Purpose Only	https://rth.dk/resources/rnp/tmRDB/
	SRPDB	Research Purpose Only	https://rth.dk/resources/rnp/SRPDB/
	tRNADB		http://trna.bioinf.uni-leipzig.de/DataOutput/
	Rnase P RFam	Public Domain CC0 1.0	https://rfam.org
	PDB	CC0 1.0	https://www.rcsb.org
Thermostability		AFL-3.0	https://benchmark.protein.properties/
Contact Map	ProteinNet	MIT	https://github.com/aqlaboratory/proteinnet
Function EC	PDB	CC0 1.0	https://www.rcsb.org

1512
1513
1514
1515
1516
1517
1518
1519
1520
1521
1522
1523
1524
1525
1526
1527
1528
1529
1530
1531
1532
1533
1534
1535
1536
1537
1538
1539
1540
1541
1542
1543
1544
1545
1546
1547
1548
1549
1550
1551
1552
1553
1554
1555
1556
1557
1558
1559
1560
1561
1562
1563
1564
1565

Table 20: Dataset used in this work(Part 2)

Dataset	Sub-dataset	License	URL
	SWISS-MODEL	CC BY-SA 4.0 Creative Commons Attribution-ShareAlike 4.0 International License	https://swissmodel.expasy.org/
Enhancer Promoter Interaction	EPIANN		https://github.com/wgmao/EP_IANN
siRNA Efficiency	Shanghai Academy of AI for Science		http://competition.sais.com.cn/
Antibody-Antigen Neutralizability	CoVAbDab	CC-BY 4.0 license	https://opig.stats.ox.ac.uk/webapps/covabdab/
	CATNAP	Non Commerical	https://www.hiv.lanl.gov/components/sequence/HIV/neutralization/download_db.comp
RNA-Protein Interaction	NPInter2.0		http://www.bioinfo.org/NPInter
	RPI7317		https://github.com/NWPU-903PR/LPI_BLS
CRISPR Off Target	DeepCRISPR	Apache-2.0 license	https://github.com/bm2-lab/DeepCRISPR
Protein-CDS-Fluorescence	NCBI		https://www.ncbi.nlm.nih.gov/bioproject/PRJNA282342
Protein-CDS-EC	ENA		https://www.ebi.ac.uk/ena
Protein-CDS-Beta Lactamase (Complete)			https://github.com/FowlerLab/Envision2017
DNA-Protein Structure	JASPAR	Creative Commons Attribution 4.0 International License.	https://jaspar.elixir.no
	HOCOMOCO		https://hocomoco11.autosome.org/